A State Alignment-Centric Approach to Federated System Identification: The FedAlign Framework

Ertuğrul Keçeci[1], Müjde Güzelkaya[1], Tufan Kumbasar[2]

[1]Faculty of Electrical and Electronics Engineering, Istanbul Technical University, Istanbul, Türkiye.
[2]Artificial Intelligence and Intelligent Systems Laboratory, Istanbul Technical University, Istanbul, Türkiye.

Contributing authors: kececie@itu.edu.tr; guzelkaya@itu.edu.tr; kumbasart@itu.edu.tr;

Abstract

This paper presents FedAlign, a Federated Learning (FL) framework particularly designed for System Identification (SYSID) tasks by aligning state representations. Local workers can learn State-Space Models (SSMs) with equivalent representations but different dynamics. We demonstrate that directly aggregating these local SSMs via FedAvg results in a global model with altered system dynamics. FedAlign overcomes this problem by employing similarity transformation matrices to align state representations of local SSMs, thereby establishing a common parameter basin that retains the dynamics of local SSMs. FedAlign computes similarity transformation matrices via two distinct approaches: FedAlign-A and FedAlign-O. In FedAlign-A, we represent the global SSM in controllable canonical form (CCF). We apply control theory to analytically derive similarity transformation matrices that convert each local SSM into this form. Yet, establishing global SSM in CCF brings additional alignment challenges in multi input - multi output SYSID as CCF representation is not unique, unlike in single input - single output SYSID. In FedAlign-O, we address these alignment challenges by reformulating the local parameter basin alignment problem as an optimization task. We determine the parameter basin of a local worker as the common parameter basin and solve least square problems to obtain similarity transformation matrices needed to align the remaining local SSMs. Through the experiments conducted on synthetic and real-world datasets, we show that FedAlign outperforms FedAvg, converges faster, and provides improved stability of the global SSM thanks to the efficient alignment of local parameter basins.

Keywords: federated learning, state alignment, deep learning, system identification

1

1 Introduction

The primary objective of the System Identification (SYSID) problem is to represent system behaviors based on time-series data by estimating a model [1, 2]. Although recent research has begun integrating machine learning models into the SYSID to represent complex system dynamics [3, 4], State Space Model (SSM) estimation techniques remain popular in SYSID. This is largely due to their reliance on linear relationships and the availability of robust, well-established estimation methods [5, 6]. Historically, SYSID studies have used data from a single source, but emerging studies indicate that sample efficiency can be boosted by employing multiple data sources from systems with analogous dynamics [7–9].

Federated Learning (FL) facilitates the training of a global model through decentralized clients, each utilizing their private data to train local models, while these models are merged and redistributed within the center server. FL naturally offers a suitable framework specifically for SYSID tasks, involving multiple time-series data collected from similar systems. [10] is the first work to incorporate the SYSID problem of multiple systems into the FL framework. The study [11] addresses the system heterogeneity through learning multiple global models based on prior dataset knowledge, whereas [12] learns multiple global models without relying on prior knowledge of datasets by utilizing an incremental clustering approach. Although the alignment problem of independently trained neural networks has been studied [13], this problem remains unaddressed in the FL-SYSID framework.

In this paper, we introduce FedAlign, an FL framework tailored for SYSID tasks by aligning state representations. We show that direct aggregation of local SSMs with equivalent representations, i.e. different parameter basins with identical dynamics, via FedAvg leads to distorted global SSM dynamics due to misaligned local parameter basins. FedAlign addresses this problem by aligning state representations of local SSMs. FedAlign establishes a common parameter basin for the global SSM in the center server and utilizes similarity transformation matrices to convert parameter basins of local SSMs into the common parameter basin. By aligning local parameter basins, FedAlign assures that the global SSM maintains the dynamics of local SSMs. FedAlign offers two distinct methods to compute similarity transformation matrices in the FL-SYSID framework:

- FedAlign-A: We depict the global SSM within the controllable canonical form (CCF). We utilize well-established linear control theory to analytically derive similarity transformation matrices that convert local SSMs into CCF representation.
- FedAlign-O: We address local parameter alignment challenges as an optimization-based problem. We set the parameter basin of a local worker as the common parameter basin. We solve least square problems using generated pseudo data to compute similarity transformation matrices, aligning remaining local SSMs with the common parameter basin. It is important to note that FedAlign-O does not determine any strict form for the global SSM.

For both FedAlign-A and FedAlign-O, we present all the design details for solving the SYSID problems of Single-Input Single-Output (SISO) and Multi-Input Multi-Output (MIMO) systems. While using MIMO data, FedAlign-A provides additional

alignment challenges as the CCF is not unique for MIMO systems, in contrast to SISO systems. However, FedAlign-O mitigates these challenges by not strictly forcing the CCF representation for the global SSM.

To validate the proposed FL-SYSID frameworks, we present comprehensive comparative results on synthetic and real-world SYSID datasets. We start by analyzing the two possible alignment challenges faced during SYSID problems. Through experiments carried out on the synthetic SISO dataset, we evaluated how local SYSID performance impacts FL-SYSID effectiveness. Moreover, we assess the impact of different creations of similarity transformation matrices on the SYSID performance of FedAlign by using two synthetic MIMO datasets. Finally, we compare the SYSID performances of FedAlign and FedAvg on the real-world SISO and MIMO datasets, illustrating that FedAlign achieves higher performance while converging faster and improving global SSM's stability thanks to effective local parameter basin alignment.

The paper is organized as follows: Section 2 gives an overview of SYSID. Section 3 addresses the alignment issues within the FL-SYSID framework by using similarity transformation matrices. Section 4 introduces the complete proposed FedAlign framework, including the design steps of FedAlign-A and FedAlign-O. Section 5 provides comprehensive comparative analyses of FedAlign. Section 6 presents the drawn conclusions as well as suggestions for future work.

2 Problem Definition of System Identification

Consider the following nonlinear system

$$
\begin{aligned}
\boldsymbol{x}_{k+1} &= f(\boldsymbol{x}_k, \boldsymbol{u}_k, \boldsymbol{w}_k) \\
\boldsymbol{y}_k &= h(\boldsymbol{x}_k, \boldsymbol{u}_k, \boldsymbol{v}_k), \quad k = 1, 2, \ldots, K
\end{aligned}
\tag{1}
$$

where $\boldsymbol{x}_k = (x_{1,k}, \ldots, x_{nx,k})^T$ represents the state vector, $\boldsymbol{u}_k = (u_{1,k}, \ldots, u_{nu,k})^T$ denotes the input vector, $\boldsymbol{y}_k = (y_{1,k}, \ldots, y_{ny,t})^T$ refers the output vector with $\boldsymbol{w}_k = (w_{1,k}, \ldots, w_{nx,t})^T$ and $\boldsymbol{v}_k = (v_{1,k}, \ldots, v_{ny,t})^T$ being input and output noises, respectively. The functions $f(\cdot)$ and $h(\cdot)$ capture the nonlinearities.

In an SYSID problem with a dataset $D = \{\boldsymbol{u}, \boldsymbol{y}\}$, (1) can be approximated by an SSM as

$$
\begin{aligned}
\tilde{\boldsymbol{x}}_{k+1} &= \tilde{A}\tilde{\boldsymbol{x}}_k + \tilde{B}\boldsymbol{u}_k, \quad \tilde{\boldsymbol{x}}_1 = \boldsymbol{x}_1 \\
\tilde{\boldsymbol{y}}_k &= \tilde{C}\tilde{\boldsymbol{x}}_k + \tilde{D}\boldsymbol{u}_k, \quad k = 1, 2, \ldots, K
\end{aligned}
\tag{2}
$$

where $\tilde{\boldsymbol{x}}_{\boldsymbol{k}}$ refers estimated states while $\tilde{\boldsymbol{y}}_{\boldsymbol{k}}$ refers estimated outputs. In (2), the state, input, output and feedthrough matrices are denoted by $\tilde{A} \in \mathbb{R}^{nx \times nx}$, $\tilde{B} \in \mathbb{R}^{nx \times nu}$, $\tilde{C} \in \mathbb{R}^{ny \times nx}$, and $\tilde{D} \in \mathbb{R}^{ny \times nu}$, respectively. Prediction Error Minimization (PEM) or N4SID methods [5, 6] can be utilized to identify these system matrices, given as $\tilde{\Theta} = \{\tilde{A}, \tilde{B}, \tilde{C}, \tilde{D}\}$. For a comprehensive discussion on SYSID, we direct readers to [1].

3 The Alignment Problem of FL-SYSID

We begin by showing that in an FL framework, the aggregation process of local SSMs with different parameter basins leads to the global model, exhibiting altered system

dynamics. Following that, we demonstrate that a common-parameter basin can be formed by aligning state representations of local SSMs leveraging similarity transformation matrices. When local SSMs are aggregated in this common parameter basin, inherent system characteristics of local SSMs are maintained in the global SSM.

3.1 The Impact of Local Parameter Basin Differences

An FL-SYSID framework involves M decentralized local workers, learning SYSID tasks using their private datasets $\boldsymbol{D} = \{D^1, D^2, \ldots, D^M\}$. Following local training at each communication round, local workers send their models to the center server. These local SSMs are aggregated via well-known FedAvg [14] to calculate the global SSM as follows:

$$\tilde{\Theta} = \frac{1}{M} \sum_{i=1}^{M} \tilde{\Theta}^{(i)} \tag{3}$$

where $\tilde{\Theta}^{(i)}$ and $\tilde{\Theta}$ denote system matrices of local SSM for W^i and system matrices for the global SSM, respectively. After the aggregation process, local workers receive $\tilde{\Theta}$ from the center server.

The efficiency of FedAvg relies on the assumption that local workers can learn system dynamics represented with similar or even the same parameter basins from their private datasets. Nevertheless, given the inherent nonuniqueness of SSMs in (2), an SSM can be expressed in equivalent representations exhibiting identical dynamics with distinct parameter basins, e.g. Controllable Canonical Form (CCF) and Observable Canonical Form (OCF). If local SSMs are in these equivalent representations, directly averaging these models as in FedAvg, may result in a global SSM with different system properties such as system gain, time-domain response, eigenvalues, controllability, and observability, potentially leading to an unstable model.

Analysis 1. Consider a FedAvg framework with two local workers to demonstrate how different parameter basins affect the global SSM dynamics. Assume local SSMs of W^1 and W^2 are in equivalent representations but with different parameter basins, W^1 in CCF and W^2 in OCF. Their state matrices are expressed as:

$$\tilde{A}^{(1)} = \begin{bmatrix} 0 & 1 & 0 \\ 0 & 0 & 1 \\ -a_3 & -a_2 & -a_1 \end{bmatrix}, \tilde{A}^{(2)} = \begin{bmatrix} 0 & 0 & -a_3 \\ 1 & 0 & -a_2 \\ 0 & 1 & -a_1 \end{bmatrix} \tag{4}$$

where the coefficients a_1, a_2, and a_3 define the characteristic polynomial

$$p(\lambda) = \det(\lambda I - A) = 0, \tag{5}$$

whose roots are the eigenvalues (λ) of the SSMs. When calculating the state matrix of the global SSM, $\tilde{A}$, through direct averaging:

$$\tilde{A} = \frac{\tilde{A}^{(1)} + \tilde{A}^{(2)}}{2} = \begin{bmatrix} 0 & 0.5 & -\frac{a_3}{2} \\ 0.5 & 0 & \frac{(1-a_2)}{2} \\ -\frac{a_3}{2} & \frac{(1-a_2)}{2} & -a_1 \end{bmatrix} \tag{6}$$

the characteristic equation of $\tilde{A}$ will differ from those of the local SSMs, causing a global SSM with altered dynamics. As a result, the global SSM may become unstable even when the individual local SSMs are stable, highlighting the risk of directly averaging equivalent SSMs with different parameter basins.

Although **Analysis-1** illustrates an edge case, it clearly demonstrates the issues of aggregating equivalent local SSMs. It shows that FedAvg can obtain global SSM with altered dynamics and jeopardize the global SSM's stability. Therefore, a local parameter basin alignment process must be used before computing the global SSM via FedAvg.

3.2 Aligning Local Parameter Basins

A similar challenge for neural networks has been addressed in [13]. The authors focus on L-layer MLP defined as:

$$f(x,\Theta) = z_{L+1}, \ z_{l+1} = \sigma(\Theta_{W_l} z_l + \Theta_{b_l}), \ z_1 = x. \tag{7}$$

where Θ is the weights set and σ refers to the activation function. They demonstrate that by applying a permutation matrix P to the weights and biases,

$$\Theta'_{W_l} = P\Theta_{W_l}, \ \Theta'_{b_l} = P\Theta_{b_l}, \ \Theta'_{W_{l+1}} = \Theta_{W_{l+1}} P^T \tag{8}$$

the transformed model, Θ', remains functionally equivalent, i.e. $f(x,\Theta) = f(x,\Theta')$. The paper introduces various techniques to calculate P that align different parameter basins into a common parameter basin. However, these methods are unsuitable for SSMs, as aligning state representations is necessary when transforming different parameter basins.

Analysis 1 depicted that the global SSM exhibits altered system dynamics when local SSMs represented through different parameter basins are aggregated. Aligning state representations of local SSMs is a must to form a common parameter basin. Instead of focusing on aligning local parameters, similarity transformation between state vectors of local SSMs can be utilized. A state vector $\boldsymbol{x}$ is transformed to alternative representation by

$$\boldsymbol{x} = T\boldsymbol{x'} \tag{9}$$

where T and $\boldsymbol{x'}$ are similarity transformation matrix and transformed state vector, respectively.

Analysis 2. In the same FL setup from Analysis 1, where local SSMs exhibit identical dynamics, a linear transformation between $\tilde{\boldsymbol{x}}^{(2)}$ and $\tilde{\boldsymbol{x}}^{(1)}$ is defined by

$$\tilde{\boldsymbol{x}}^{(2)} = T\tilde{\boldsymbol{x}}^{(1)} \tag{10}$$

with T being any nonsingular matrix, known as similarity transformation [15] (Section 4 will introduce two distinct methods to compute T). A common parameter basin is

5

formed by aligning state vectors with (10), linking $\tilde{\Theta}^{(1)}$ and $\tilde{\Theta}^{(2)}$ through the following equations.

$$\tilde{A}^{(1)} = T^{-1}\tilde{A}^{(2)}T, \quad \tilde{B}^{(1)} = T^{-1}\tilde{B}^{(2)}$$
$$\tilde{C}^{(1)} = \tilde{C}^{(2)}T, \quad \tilde{D}^{(1)} = \tilde{D}^{(2)} \tag{11}$$

Subsequently, the global SSM, $\tilde{\Theta} = \{\tilde{A}, \tilde{B}, \tilde{C}, \tilde{D}\}$ is calculated as follows:

$$\tilde{A} = \frac{\tilde{A}^{(1)} + T^{-1}\tilde{A}^{(2)}T}{2}, \quad \tilde{B} = \frac{\tilde{B}^{(1)} + T^{-1}\tilde{B}^{(2)}}{2},$$
$$\tilde{C} = \frac{\tilde{C}^{(1)} + \tilde{C}^{(2)}T}{2}, \quad \tilde{D} = \frac{\tilde{D}^{(1)} + \tilde{D}^{(2)}}{2}. \tag{12}$$

The resulting state matrix for the global SSM takes the following form:

$$\tilde{A} = \begin{bmatrix} 0 & 1 & 0 \\ 0 & 0 & 1 \\ -a_3 & -a_2 & -a_1 \end{bmatrix}, \tag{13}$$

We illustrated that the CCF representation on the common parameter basin is maintained for the global SSM. In contrast to the merging by direct averaging, as in (3), the global SSM obtained with (11) preserves the same dynamics as local SSMs. Furthermore, the global SSM maintains identical eigenvalues as the local SSMs, thereby guaranteeing stability if the local SSMs are stable thanks to the state representation alignment of the local SSMs.

4 FedAlign: The FL framework for SYSID tasks

This section introduces the FedAlign framework that builds a global SSM by aligning state representations of local SSMs, ensuring the global SSM exhibits similar dynamics to those of local SSMs. FedAlign accomplishes this by leveraging similarity transformation matrices. During each communication round, the center server employs similarity transformations (T) to form a common parameter basin. It then computes a global SSM that retains the properties of local SSMs by averaging them within this common parameter basin.

$$\tilde{A} = \frac{1}{M}\sum_{i=1}^{M} T_i^{-1}\tilde{A}^{(i)}T_i, \quad \tilde{B} = \frac{1}{M}\sum_{i=1}^{M} T_i^{-1}\tilde{B}^{(i)}$$
$$\tilde{C} = \frac{1}{M}\sum_{i=1}^{M} \tilde{C}^{(i)}T_i, \quad \tilde{D} = \frac{1}{M}\sum_{i=1}^{M} \tilde{D}^{(i)} \tag{14}$$

Algorithm 1 FedAlign

1: **Initialization:** number of communication rounds R, local iterations *iter*, initialize local SSM parameters $\tilde{\Theta}_0^{(i)}$ for each worker W^i, $\forall i \in [M]$
2: Choose alignment method: **FedAlign-A** or **FedAlign-O**
3: **for** $r = 0, 1, 2, \ldots, R-1$ **do**
4:     Server broadcasts current local SSM parameters $\tilde{\Theta}_r^{(i)}$ to local workers
5:     **for** each local worker W^i **in parallel do**
6:         $\tilde{\Theta}_{r+1}^{(i)} \leftarrow \textbf{LocalUpdate}(\tilde{\Theta}_r^{(i)}, iter)$
7:         Send updated local parameters $\tilde{\Theta}_{r+1}^{(i)}$ to server
8:     **end for**
9:     Compute T_i, $\forall i \in [M]$ (using FedAlign-A or FedAlign-O)
10:     Aggregate aligned local SSMs to obtain $\tilde{\Theta}_{r+1}$ (using (14))
11:     Obtain $\tilde{\Theta}_{r+1}^{(i)}$, $\forall i \in [M]$ (using (15))
12:     Server sends $\tilde{\Theta}_{r+1}^{(i)}$ back to respective workers
13: **end for**

At the end of each communication round, the center server converts the global SSM on the common parameter basin to the local basin of each local SSM with

$$\tilde{A}^{(i)} = T_i \tilde{A} T_i^{-1}, \quad \tilde{B}^{(i)} = T_i \tilde{B}$$
$$\tilde{C}^{(i)} = \tilde{C} T_i^{-1}, \quad \tilde{D}^{(i)} = \tilde{D} \tag{15}$$

Afterward, it sends the updated local SSMs to their respective local workers. Algorithm 1[1] provides a detailed overview of FedAlign's training procedure.

In this paper, we propose two methods for calculating T within the FL-SYSID framework: 1) FedAlign-A, a data-free analytical approach, and 2) FedAlign-O, a data-driven optimization-based method.

4.1 FedAlign-A: the Analytical Method

In FedAlign-A, we represent the common parameter basin within the CCF for the global SSM. Hence, we convert the local parameter basin of each local SSM into the CCF. It is worth noting that CCF is an option, any equivalent representation could be used. Moreover, for SISO ($nu = ny = 1$) and MIMO ($nu, ny > 1$) systems, we calculate similarity transformations using different mathematical formulations.

---

[1]MATLAB implementation. [Online]. Available: Github repo will be shared upon the acceptance of the paper

4.1.1 FedAlign-A for SISO SYSID

For SISO SYSID tasks, upon completion of local training, the center server computes T_i, aligning the local parameter basin of W^i with the CCF representation using:

$$
T_i = P^{(i)} \begin{bmatrix} a_1 & a_2 & \cdots & a_{nx-1} & 1 \\ a_2 & a_3 & \cdots & 1 & 0 \\ \vdots & \vdots & \ddots & \vdots & \vdots \\ a_{nx-1} & 1 & \cdots & 0 & 0 \\ 1 & 0 & \cdots & 0 & 0 \end{bmatrix}. \tag{16}
$$

Here, the controllability matrix is denoted by $P^{(i)} = [\tilde{B}^{(i)} \ \tilde{A}^{(i)}\tilde{B}^{(i)} \ \ldots \ (\tilde{A}^{(i)})^{nx-1}\tilde{B}^{(i)}]$ whereas $a_1, a_2, \ldots, a_{nx-1}$ refer the coefficient of the $p(\lambda)$ for W^i.

4.1.2 FedAlign-A for MIMO SYSID

Similar to the SISO case, T_i is calculated by the center server after local training. Yet, calculating T_i is more challenging and is not unique for MIMO systems [16].

To define T_i, let us first express the input matrix of W^i as:

$$
\tilde{B}^{(i)} = \begin{bmatrix} \tilde{b}_1^{(i)} & \tilde{b}_2^{(i)} & \cdots & \tilde{b}_{nu}^{(i)} \end{bmatrix}, \tag{17}
$$

where $\tilde{b}_\ell^{(i)}$ is the column representing ℓ^{th} input ($\ell = 1, 2, \ldots, nu$). The controllability matrix is

$$
P^{(i)} = \begin{bmatrix} P_1^{(i)} & P_2^{(i)} & \cdots & P_{nu}^{(i)} \end{bmatrix} \tag{18}
$$

where each block is defined as

$$
P_\ell^{(i)} = \begin{bmatrix} \tilde{b}_\ell^{(i)} & \tilde{A}^{(i)}\tilde{b}_\ell^{(i)} & \cdots & \left(\tilde{A}^{(i)}\right)^{nx-1} \tilde{b}_\ell^{(i)} \end{bmatrix}. \tag{19}
$$

We select μ_ℓ independent column from each $P_\ell^{(i)}$ and denote this selection as matrix

$$
M^{(i)} = \Big[\underbrace{\tilde{b}_1^{(i)} \quad \tilde{A}^{(i)}\tilde{b}_1^{(i)} \quad \cdots \quad (\tilde{A}^{(i)})^{\mu_1-1}\tilde{b}_1^{(i)}}_{\mu_1 \text{ columns}},
$$
$$
\cdots ,
$$
$$
\underbrace{\tilde{b}_{nu}^{(i)} \quad \tilde{A}^{(i)}\tilde{b}_{nu}^{(i)} \quad \cdots \quad (\tilde{A}^{(i)})^{\mu_{nu}-1}\tilde{b}_{nu}^{(i)}}_{\mu_{nu} \text{ columns}} \Big] \tag{20}
$$

8

where $\sum_{\ell=1}^{nu} \mu_\ell = nx$. We define the inverse of $M^{(i)}$ with row vectors $m^{(i)}$ as follows:

$$
\left(M^{(i)}\right)^{-1} = \begin{bmatrix}
m_{1,1}^{(i)} \\
m_{1,2}^{(i)} \\
\vdots \\
m_{1,\mu_1}^{(i)} \\
\hline
\vdots \\
\hline
m_{nu,1}^{(i)} \\
m_{nu,2}^{(i)} \\
\vdots \\
m_{nu,\mu_{nu}}^{(i)}
\end{bmatrix}.
$$

Then, we calculate T_i by using the last row from each partition, the rows denoted $m_{\ell,\mu_{nu}}$ for $\ell = 1, 2, \ldots, nu$ [16].

$$
T_i = \begin{bmatrix}
m_{1,\mu_1}^{(i)} \\
m_{1,\mu_1}^{(i)} \tilde{A}^{(i)} \\
\vdots \\
m_{1,\mu_1}^{(i)} \left(\tilde{A}^{(i)}\right)^{\mu_1 - 1} \\
\hline
\vdots \\
\hline
m_{nu,\mu_{nu}}^{(i)} \\
m_{nu,\mu_{nu}}^{(i)} \tilde{A}^{(i)} \\
\vdots \\
m_{nu,\mu_{nu}}^{(i)} \left(\tilde{A}^{(i)}\right)^{\mu_{nu} - 1}
\end{bmatrix}^{-1}
\tag{21}
$$

In the MIMO case of FedAlign-A, CCF transformation introduces an additional challenge due to its non-uniqueness. The structural hyperparameter μ_ℓ must be set before training, as different choices of μ_ℓ lead to distinct representations of T_i. This variability impacts how local SSMs align, influencing the stability and accuracy of the global SSM. Certain settings of μ_ℓ may result in T_i with high condition numbers ($\kappa(T_i)$), which can affect numerical stability and lead to deviations in system dynamics after similarity transformation. Thus, the choice of μ_ℓ is critical for achieving effective state alignment, essential for ensuring stable and accurate SYSID.

4.2 FedAlign-O: the Optimization-based Method

To overcome the challenges of aligning all local workers through the transformation into CCF, we propose FedAlign-O, which treats the alignment problem as an optimization task, making it suitable for both SISO and MIMO SYSID tasks.

In FedAlign-O, instead of forcing strict representation (such as CCF in FedAlign-A), we randomly pick an index $j \in [M]$ and designate the parameter basin of W^j as the common parameter basin for the global SSM. We align the remaining workers' state representations with the state representation of W^j. To achieve this, the center server solves the following least squares problem to estimate each T_i via generated pseudo-states for each W^i ($\tilde{\boldsymbol{x}}_{pseudo}^{(i)}$).

$$T_i = \underset{T}{\arg\min} \sum (\tilde{\boldsymbol{x}}_{pseudo}^{(i)} - T\tilde{\boldsymbol{x}}_{pseudo}^{(j)})^2, \forall i \neq j. \tag{22}$$

Note that we define $T_j = I_{nx}$ as the parameter basin of W^j defines the common parameter basin.

FedAlign-O addresses potential structural issues with T_i that may arise in FedAlign-A by not enforcing all local workers to be represented in CCF. It also eliminates the need for the μ_ℓ setting in MIMO SYSID. However, it requires the availability of an extra dataset or the generation of pseudo-data at the central server.

5 Comparative Performance Analysis

We present extensive experimental results on the SYSID performance of FL-SYSID using FedAlign-A and FedAlign-O compared to FedAvg. Each FL framework utilized the same training configuration, comprising $M = 20$ workers for $R = 20$ communication rounds. PEM was employed for local SYSID with two hyperparameters: model order nx and local iteration $iter$. All experiments were conducted in MATLAB® and repeated with 20 different seeds for statistical analysis.

For each experiment, the overall SYSID performance is assessed by averaging the Best Fit Rate (BFR) of each local worker W^i, $i \in [M]$. For an output, BFR is computed as:

$$\text{BFR}_p = \frac{1}{M} \sum_{i \in [M]} \text{BFR}_p^{(i)}. \tag{23}$$

Here, the Best Fit Rate $\text{BFR}_p^{(i)}$ for local worker W^i is defined by

$$\text{BFR}_p^{(i)} = 100 \left(1 - \sqrt{\frac{\sum_{k=1}^{K} \left(y_{p,k}^{(i)} - \tilde{y}_{p,k}^{(i)}\right)^2}{\sum_{k=1}^{K} \left(y_{p,k}^{(i)} - \bar{y}_p^{(i)}\right)^2}} \right), \tag{24}$$

where $\bar{y}_p^{(i)} = (1\backslash K) \sum_{k=1}^{K} y_{p,k}^{(i)}$ and $p = 1, 2, \ldots, ny$. We also recorded the total number of unstable global SSMs (#UM) to assess the impact of direct averaging on global SSM stability. Additionally, we tracked the total number of global SSMs that failed to learn (#F2L), defined as those with a BFR below zero. Experiments resulting in unstable or failed-to-learn global SSMs were excluded from BFR calculations.

The investigation consists of a four-fold statistical analysis:

- **Section 5.1:** To assess the impact of local SYSID performance on the efficiency of FL-SYSID, we conducted experiments on a synthetic SISO dataset using different values of *iter* and *nx*.
- **Section 5.2:** We analyzed how the choice of μ_ℓ affects the numerical stability of T_i generated by FedAlign-A across two synthetic MIMO datasets with distinct dynamics. By exploring various μ_ℓ settings, we evaluated their influence on the efficiency of FedAlign-A.
- **Sections 5.3 and 5.4:** We conducted experiments on real-world SISO and MIMO datasets to compare the SYSID performance of FedAlign and FedAvg on both training and test data.

5.1 Analyzing Alignment Challenges resulting from local SYSID performance

We created a synthetic dataset from a third-order system with zero dynamics ($nu = ny = 1$). We sampled the initial states, inputs, and input noises as $\boldsymbol{x}_1^{(i)} \sim \mathcal{N}(0, 0.1^2 I_{nx})$, $\boldsymbol{u}_{1:K}^{(i)} \sim \mathcal{N}(0, 0.1^2 I_{nu})$, $\boldsymbol{w}_{1:K}^{(i)} \sim \mathcal{N}(0, 0.003^2 I_{nx})$, respectively. We attached a distinct dataset $D^i = \{\boldsymbol{u}^{(i)}, \boldsymbol{y}^{(i)}\}$ to each W^i.

To analyze local SYSID performances on FL-SYSID, we set $nx = \{2, 3\}$ and $iter = \{1, 20\}$ for the local SSMs in the analysis. It should be pointed that, despite the actual system being third order ($nx = 3$), we set $nx = 2$ to assess reduced order modeling performance. We generated $\tilde{\boldsymbol{x}}_{pseudo}^{(i)}$ in FedAlign-O with $\boldsymbol{u}_{1:K}^{(i)} \sim \mathcal{N}(0, 1^2 I_{nu})$.

The mean BFR values with standard errors, #UM, and #F2L over 20 experiments are reported in Table 1. The box plots of $BFR^{(i)}$ are given in Fig. 1 and the $BFR^{(i)}$ during training are given in Fig. 2. Based on the results, we conclude that:

- FedAlign performs constantly better than FedAvg for the $nx = 3$ and $iter = 1$ settings. FedAvg requires a higher number of local iterations ($iter = 20$) to match the performance of FedAlign.
- With the reduced-order learning model ($nx = 2$), all methods experience a decrease in SYSID performance. As shown in Fig. 1, FedAvg evaluates lower performance

Table 1 Analysis of Local SYSID Performance in FL-SYSID Across 20 Experiments

		FedAvg		FedAlign-A		FedAlign-O	
		iter=1	iter=20	iter=1	iter=20	iter=1	iter=20
	BFR$_1$	55.47($\pm$28.17)	74.05($\pm$0.48)	74.05($\pm$0.44)	74.05($\pm$0.44)	74.05($\pm$0.44)	74.04($\pm$0.44)
$nx = 2$	**#UM**	1	1	0	0	0	0
	#F2L	0	0	0	0	0	0
	BFR$_1$	57.91($\pm$29.34)	83.53($\pm$0.32)	83.50($\pm$0.33)	83.51($\pm$0.32)	83.50($\pm$0.32)	83.51($\pm$0.32)
$nx = 3$	**#UM**	3	2	0	0	0	0
	#F2L	0	0	0	0	0	0

(a) $nx = 2$, $iter = 1$ (b) $nx = 2$, $iter = 20$

(c) $nx = 3$, $iter = 1$ (d) $nx = 3$, $iter = 20$

Fig. 1 Box plot comparison of FedAlign and FedAvg on Synthetic Dataset

(a) $nx = 2$, $iter = 1$ (b) $nx = 2$, $iter = 20$
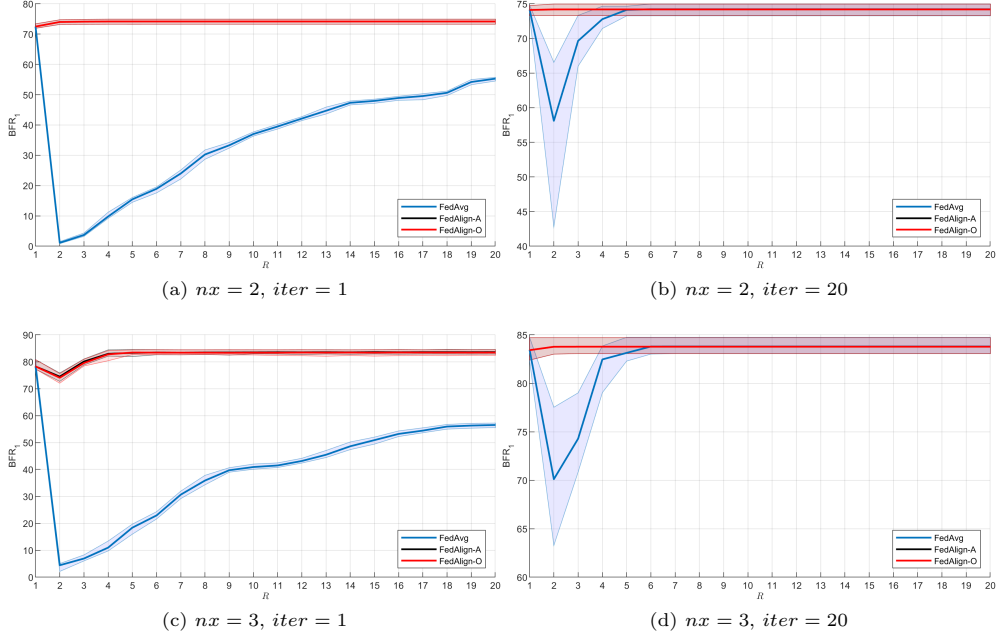
(c) $nx = 3$, $iter = 1$ (d) $nx = 3$, $iter = 20$

Fig. 2 Comparison of FedAlign and FedAvg Training on the Synthetic Dataset: Mean $\mathrm{BFR}^{(i)}$ across local workers (solid lines) and the minimum and maximum $\mathrm{BFR}^{(i)}$ across local workers (shaded areas).

with higher variability. FedAvg could only achieve a performance similar to FedAlign only when the local iteration is increased to $iter = 20$, similar to $nx = 3$ case.

- Fig. 2 illustrates that FedAvg suffers from sudden performance drops in the earlier communication rounds. Due to the alignment of local parameter basins, FedAlign does not show such decreases during training, which results in faster convergence.
- While FedAlign generates only stable global SSMs, thanks to local parameter basin alignment, FedAvg yields unstable global SSMs in all setups. Neither methods obtain F2L global SSM.
- Even though FedAlign-A does not demand pseudo-data generation to compute T_i, it achieves on-par SYSID performance with FedAlign-O. As shown in Fig. 2, it also matches the FedAlign-O's performance during training.

All in all, aligning the states of local SSMs provides several advantages to FedAlign, even with a single local iteration or reduced order modeling, including higher SYSID performance, quicker convergence, and improved global SSM stability.

5.2 Analyzing Alignment Challenges in FedAlign-A for MIMO SYSID

We generated two synthetic datasets, MIMO Synthetic dataset 1 (MIMO-1) and MIMO Synthetic dataset 2 (MIMO-2), to investigate how different T_i constructed with various μ_ℓ choices impact the SYSID performance of FedAlign-A. Both MIMO-1 and MIMO-2 are derived from fourth-order SSMs ($nx = 4$) with two inputs and two outputs ($nu = ny = 2$) exhibiting different dynamics. We sampled the initial states as $\boldsymbol{x}_1^{(i)} \sim \mathcal{N}(0, 0.1^2 I_{nx})$, the inputs as $\boldsymbol{u}_{1:K}^{(i)} \sim \mathcal{N}(0, 0.1^2 I_{nu})$, and the output noises as $\boldsymbol{w}_{1:K}^{(i)} \sim \mathcal{N}(0, 0.01^2 I_{nx})$. We assigned a unique dataset $D^i = \{\boldsymbol{u}^{(i)}, \boldsymbol{y}^{(i)}\}$ to each W^i.

In the analysis, we set $nx = 4$ and $iter = \{1, 20\}$ for the local SSMs. We utilized $\boldsymbol{u}_{1:K}^{(i)} \sim \mathcal{N}(0, 0.1^2 I_{nu})$ to generate $\tilde{\boldsymbol{x}}_{pseudo}^{(i)}$ in FedAlign-O. In FedAlign-A, we constructed $M^{(i)}$ using three different μ_ℓ settings:

- FedAlign-A1: We used only the first input by setting $\mu_1 = 4$ to construct $M^{(i)}$ as
$$M^{(i)} = \left[\tilde{b}_1^{(i)} \ \tilde{A}^{(i)}\tilde{b}_1^{(i)} \ \left(\tilde{A}^{(i)}\right)^2 \tilde{b}_1^{(i)} \ \left(\tilde{A}^{(i)}\right)^3 \tilde{b}_1^{(i)} \right]$$
- FedAlign-A2: We used only the second input by setting $\mu_2 = 4$ to construct $M^{(i)}$ as $M^{(i)} = \left[\tilde{b}_2^{(i)} \ \tilde{A}^{(i)}\tilde{b}_2^{(i)} \ \left(\tilde{A}^{(i)}\right)^2 \tilde{b}_2^{(i)} \ \left(\tilde{A}^{(i)}\right)^3 \tilde{b}_2^{(i)} \right]$,
- FedAlign-A3: We used both first and second inputs by setting $\mu_1 = \mu_2 = 2$ to construct $M^{(i)}$ as $M^{(i)} = \left[\tilde{b}_1^{(i)} \ \tilde{A}^{(i)}\tilde{b}_1^{(i)} \ \tilde{b}_2^{(i)} \ \tilde{A}^{(i)}\tilde{b}_2^{(i)} \right]$.

For all settings, we examined the resulting condition number of T_i, $\kappa(T_i)$, throughout communication rounds to examine the impacts of numerical instabilities of T_i on the efficiency of similarity transformation.

Table 2 and Table 3 present the mean BFR values with standard errors alongside #UM and #F2L for $iter = 1$ and $iter = 20$, respectively. Fig. 3 illustrates how $log(\kappa(T_i))$ changes during training in FedAlign whereas Fig. 4 and Fig. 5 display the
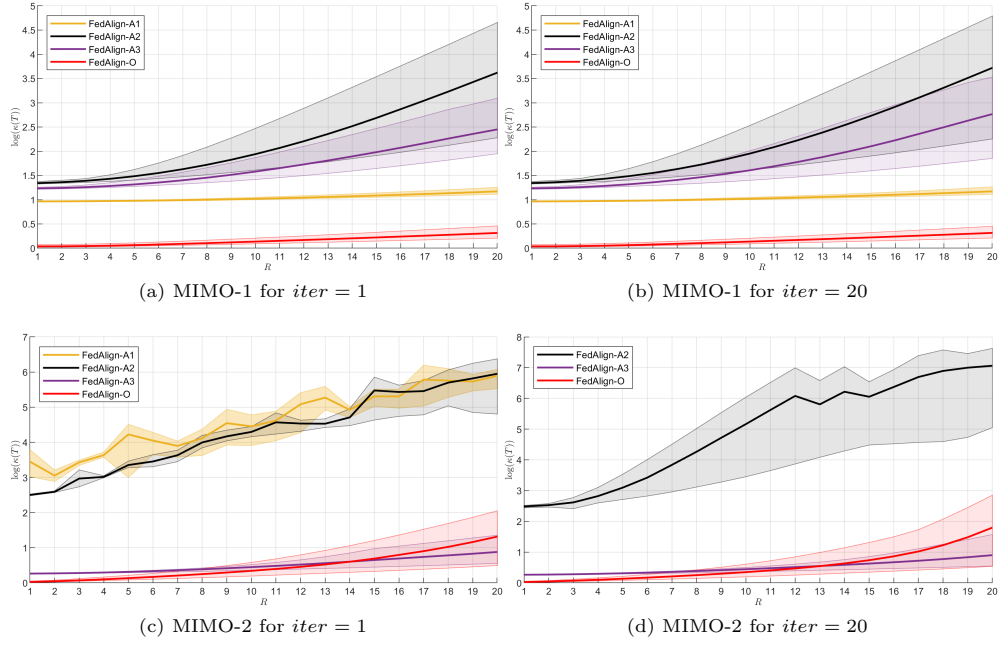
(a) MIMO-1 for $iter = 1$ (b) MIMO-1 for $iter = 20$

(c) MIMO-2 for $iter = 1$ (d) MIMO-2 for $iter = 20$

Fig. 3 Sensitivity comparison of FedAlign-A and FedAlign-O during training on the synthetic datasets: Mean $log(\kappa(T_i))$ across local workers (solid lines) and the minimum and maximum $log(\kappa(T_i))$ across local workers (shaded areas).
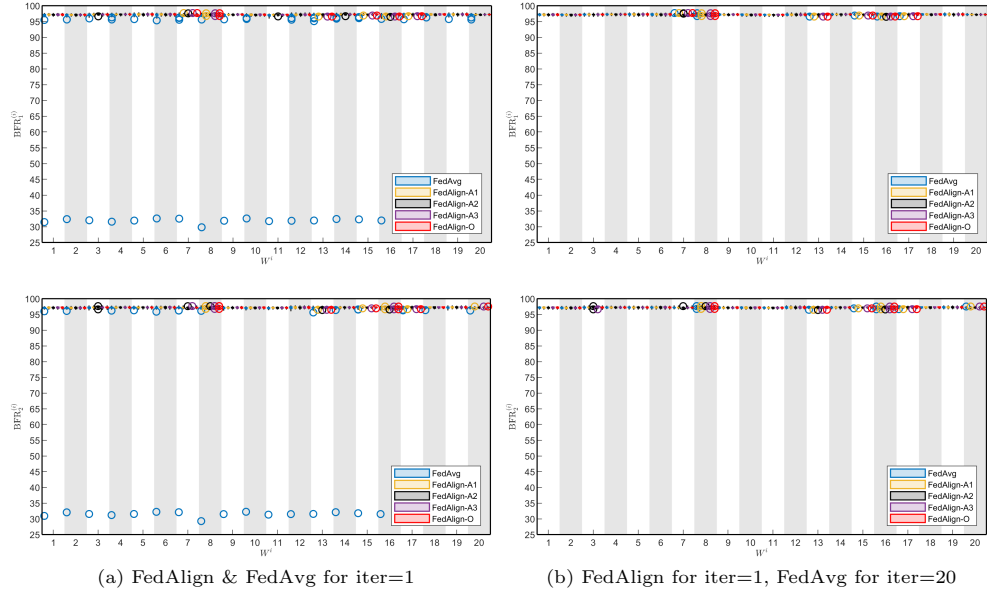

(a) FedAlign & FedAvg for iter=1   (b) FedAlign for iter=1, FedAvg for iter=20

Fig. 4 Box plot comparison of FedAlign and FedAvg on MIMO-1 dataset for two outputs y_1 (top row) and y_2 (bottom row).

14

Table 2 Analysis of local SYSID performance in FL-SYSID with $iter = 1$ across 20 experiments

		FedAvg	FedAlign-A1	FedAlign-A2	FedAlign-A3	FedAlign-O
MIMO-1	**BFR$_1$**	93.77($\pm$14.56)	97.18($\pm$0.05)	97.12($\pm$0.08)	97.18($\pm$0.05)	97.18($\pm$0.05)
	BFR$_2$	93.81($\pm$14.67)	97.17($\pm$0.06)	97.14($\pm$0.07)	97.17($\pm$0.06)	97.17($\pm$0.06)
	#UM	0	0	0	0	0
	#F2L	0	0	0	0	0
MIMO-2	**BFR$_1$**	96.87($\pm$0.09)	75.49($\pm$18.71)	63.75($\pm$41.67)	96.90($\pm$0.03)	96.90($\pm$0.03)
	BFR$_2$	96.80($\pm$0.15)	82.06($\pm$7.97)	71.19($\pm$32.97)	96.85($\pm$0.02)	96.85($\pm$0.02)
	#UM	1	8	6	0	0
	#F2L	1	9	11	0	0

Table 3 Analysis of local SYSID performance in FL-SYSID with $iter = 20$ across 20 experiments

		FedAvg	FedAlign-A1	FedAlign-A2	FedAlign-A3	FedAlign-O
MIMO-1	**BFR$_1$**	97.18($\pm$0.05)	97.18($\pm$0.05)	97.13($\pm$0.08)	97.18($\pm$0.05)	97.18($\pm$0.05)
	BFR$_2$	97.17($\pm$0.06)	97.17($\pm$0.06)	97.15($\pm$0.07)	97.17($\pm$0.06)	97.17($\pm$0.06)
	#UM	0	0	0	0	0
	#F2L	0	0	0	0	0
MIMO-2	**BFR$_1$**	96.90($\pm$0.03)	–	90.85($\pm$6.47)	96.90($\pm$0.03)	96.90($\pm$0.03)
	BFR$_2$	96.85($\pm$0.02)	–	91.70($\pm$6.99)	96.85($\pm$0.02)	96.85($\pm$0.02)
	#UM	0	20	9	0	0
	#F2L	0	0	2	0	0

box plots of BFR$^{(i)}$ for MIMO-1 and MIMO-2, respectively. Based on these findings, we observe that:

- On the MIMO-1 dataset for $iter = \{1, 20\}$, all methods ensure efficient similarity transformation by computing small $\kappa(T_i)$ as seen from Fig. 3a and Fig. 3b, thus providing high SYSID performance.
- On the MIMO-2 dataset for $iter = 1$, $\kappa(T_i)$ becomes higher in FedAlign-A1 and FedAlign-A2 while FedAlign-A3 and FedAlign-O obtain significantly lower $\kappa(T_i)$. As a result, inefficient similarity transformations in FedAlign-A1 and FedAlign-A2 lead to poor SYSID performance and the generation of unstable or F2L global SSMs. On the other hand, for $iter = 20$, FedAlign-A1 generates only unstable global SSMs whereas $\kappa(T_i)$ remains higher in FedAlign-A2, as shown in Fig. 3d.
- FedAvg evaluates fewer BFR values with higher deviation than FedAlign on the MIMO-1 dataset for $iter = 1$, and requires higher local iterations ($iter = 20$) to match FedAlign's performance, as shown in Fig. 4. However, on the MIMO-2
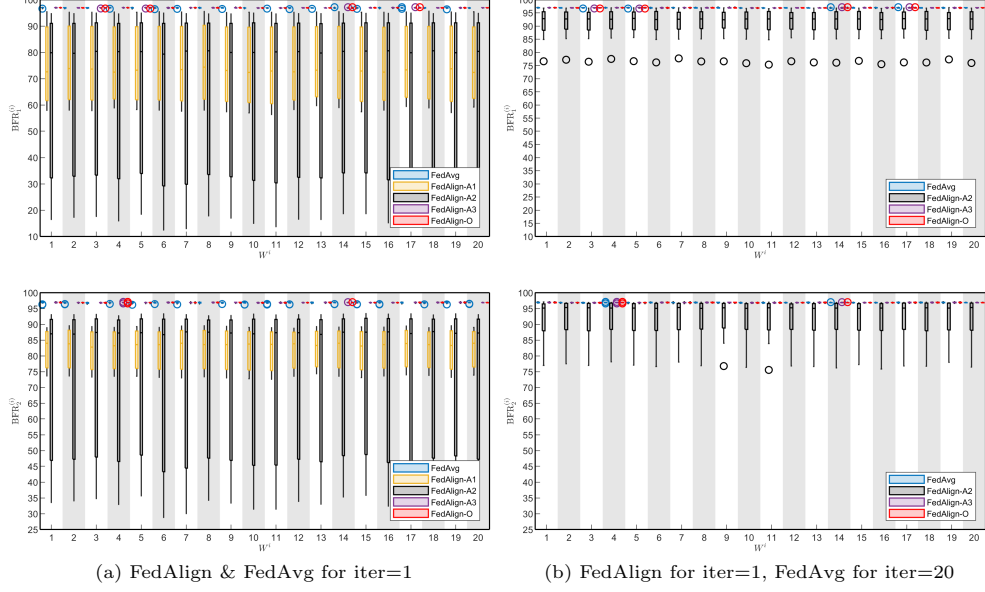
Fig. 5 Box plot comparison of FedAlign and FedAvg on MIMO-2 dataset for two outputs y_1 (top row) and y_2 (bottom row).

dataset for $iter = \{1, 20\}$, FedAvg gives higher performance than FedAlign-A1 and FedAlign-A2, and achieves performance on par with FedAlign-A3 and FedAlign-O, as depicted in Fig. 5.

In summary, FedAlign-A may yield high $\kappa(T_i)$ depending on the choice of μ_ℓ, which considerably hinders the effectiveness of local parameter basin alignment, thus implying that μ_ℓ must be set carefully. On the other hand, FedAlign-O obtains small $\kappa(T_i)$ as it does not obligate CCF representation for the global SSM.

5.3 Performance comparison study on real-world SISO datasets

We assessed the SYSID performance using the real-world SISO datasets. The datasets are pre-split into training and test subsets $D = \{D_{\text{train}}, D_{\text{test}}\}$ and listed as follows:

- MR Damper dataset [17] includes 3499 samples where velocity is the input and damper force is the output. The first 3000 samples comprise D_{train} while D_{test} contains the remaining samples. We added Gaussian noise, $\boldsymbol{v}_{1:K}^{(i)} \sim \mathcal{N}(0, 5^2)$ into D_{train} for each W^i to obtain distinct datasets.
- The Hair Dryer dataset [18] includes 1000 samples where heater voltage is the input and thermocouple voltage is the output. The first 300 samples constitute D_{train} and D_{test} contains samples 801-900. To gather zero mean data, we detrended the dataset. Moreover, we added $\boldsymbol{v}_{1:K}^{(i)} \sim \mathcal{N}(0, 0.05^2)$ into D_{train} for each W^i.
- The Piezoelectric dataset [19] includes 10,000 samples where actuator voltage is the input and displacement is the output. The first 5,000 samples form D_{train} while the

Table 4 Performance analysis over 20 experiments

			FedAvg		FedAlign-A	FedAlign-O
			iter=1	iter=20	iter=1	iter=1
MR Damper	**BFR**	Train	50.58(±2.54)	51.06(±2.04)	51.95(±0.08)	52.06(±0.08)
		Test	58.30(±2.98)	58.40(±2.86)	59.82(±0.18)	60.04(±0.07)
	#UM		0	0	0	0
	#F2L		0	0	0	0
Hair Dryer	**BFR**	Train	63.05(±22.63)	82.88(±14.73)	87.66(±0.07)	87.66(±0.07)
		Test	61.17(±24.23)	82.85(±15.97)	87.91(±0.05)	87.89(±0.05)
	#UM		1	0	0	0
	#F2L		0	0	0	0
Piezoelectric	**BFR**	Train	53.80(±5.04)	57.31(±1.44)	57.30(±1.62)	57.46(±0.92)
		Test	53.66(±5.26)	60.94(±1.81)	57.57(±1.57)	57.82(±0.98)
	#UM		0	1	0	0
	#F2L		0	0	0	0

last 5,000 samples establish D_{test}. We added $\boldsymbol{v}_{1:K}^{(i)} \sim \mathcal{N}(0, 5^2)$ into D_{train} for each W^i.

As depicted in Section 5.1, FedAlign achieves higher BFR values with fewer local iterations. Therefore, we set $iter = 1$ for FedAlign, while for FedAvg, we set $iter = \{1, 20\}$. For the MR Damper and Hair Dryer datasets, we set $nx = 3$. For the Piezoelectric dataset, we set $nx = 4$. We generated $\tilde{\boldsymbol{x}}_{pseudo}^{(i)}$ by using $\boldsymbol{u}_{1:K}^{(i)} \in D_{test}^i$ in FedAlign-O.

We reported the mean BFR values with standard errors alongside #UM and #F2L in Table 4. We also evaluated BFR using D_{test} to analyze the global SSM's performance against test data. We gave box plots of BFR$^{(i)}$ for FedAvg and FedAlign in Fig. 6. Furthermore, we illustrated the BFR$^{(i)}$ progression across communication rounds in Fig. 7. From the results, we infer that:

- For $iter = 1$, FedAlign constantly shows superior performances on all datasets as seen in Fig. 6. Although using higher local iterations ($iter = 20$) improves the performance of FedAvg, it matches FedAlign only in the Piezoelectric dataset. Even with $iter = 20$ setup, FedAvg exhibits lower performance with higher deviation in MR Damper and Hair Dryer datasets as shown in Fig. 6b and Fig. 6d.
- As demonstrated in Fig. 7, FedAlign converges faster with steady performance, whereas FedAvg displays significant performance decreases during early communication rounds.
- FedAvg obtains unstable global SSMs in the Hair Dryer and Piezoelectric datasets. On the other hand, FedAlign generates only stable global SSMs, thanks to local parameter basin alignment. Neither of the methods yields any F2L global SSM.
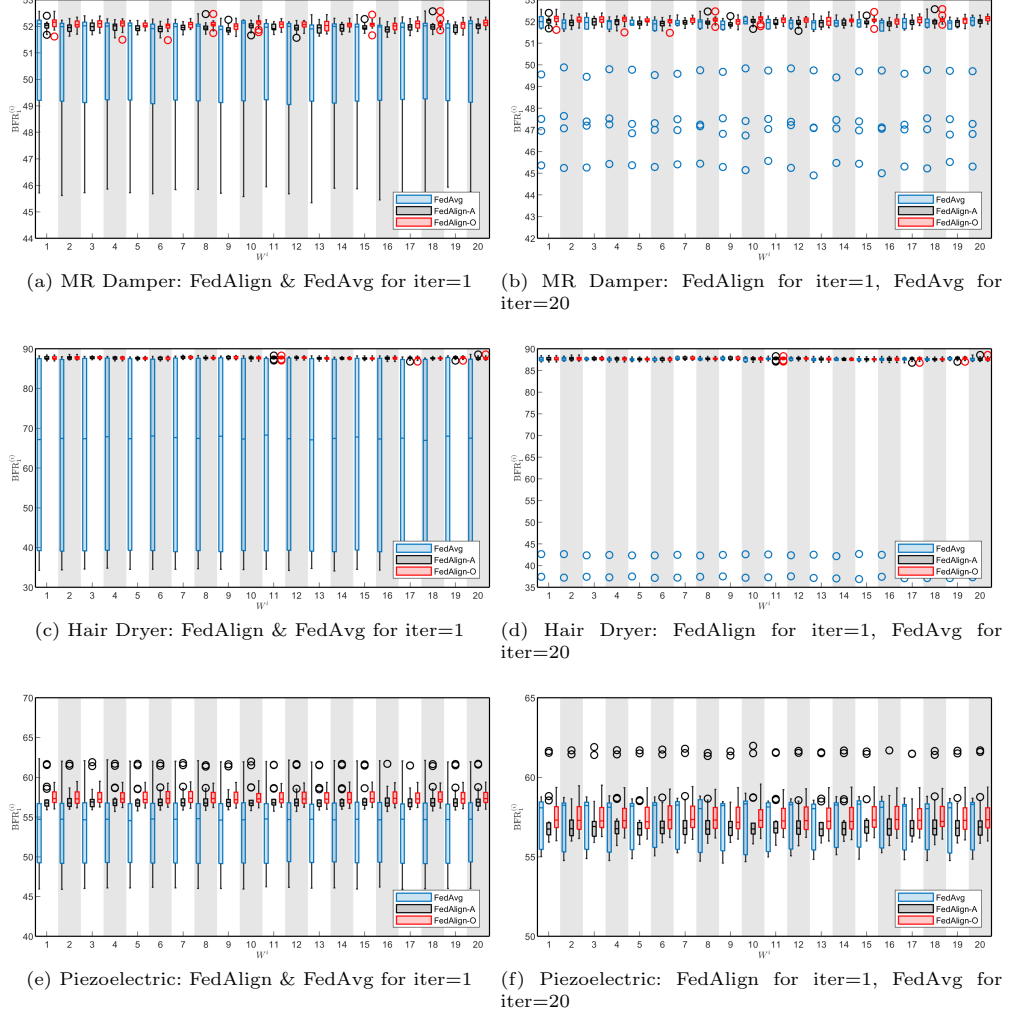
(a) MR Damper: FedAlign & FedAvg for iter=1

(b) MR Damper: FedAlign for iter=1, FedAvg for iter=20

(c) Hair Dryer: FedAlign & FedAvg for iter=1

(d) Hair Dryer: FedAlign for iter=1, FedAvg for iter=20

(e) Piezoelectric: FedAlign & FedAvg for iter=1

(f) Piezoelectric: FedAlign for iter=1, FedAvg for iter=20

Fig. 6 Box plot comparisons on real-world datasets.

- FedAlign evaluates higher test BFR in all datasets for $iter = 1$. FedAvg with $iter = 20$ outperforms FedAlign against unseen data in the Piezoelectric dataset whereas it still obtains fewer test BFR in the MR Damper and Hair Dryer datasets.
- FedAlign-A and FedAlign-O exhibit similar performances against training and test data. However, it is worth noting that, FedAlign-O deviates less in the Piezoelectric dataset.

To sum up, the efficient alignment of local parameter basins enables FedAlign to excel in both training and testing, alongside faster convergence and enhanced stability, even with fewer local iterations.
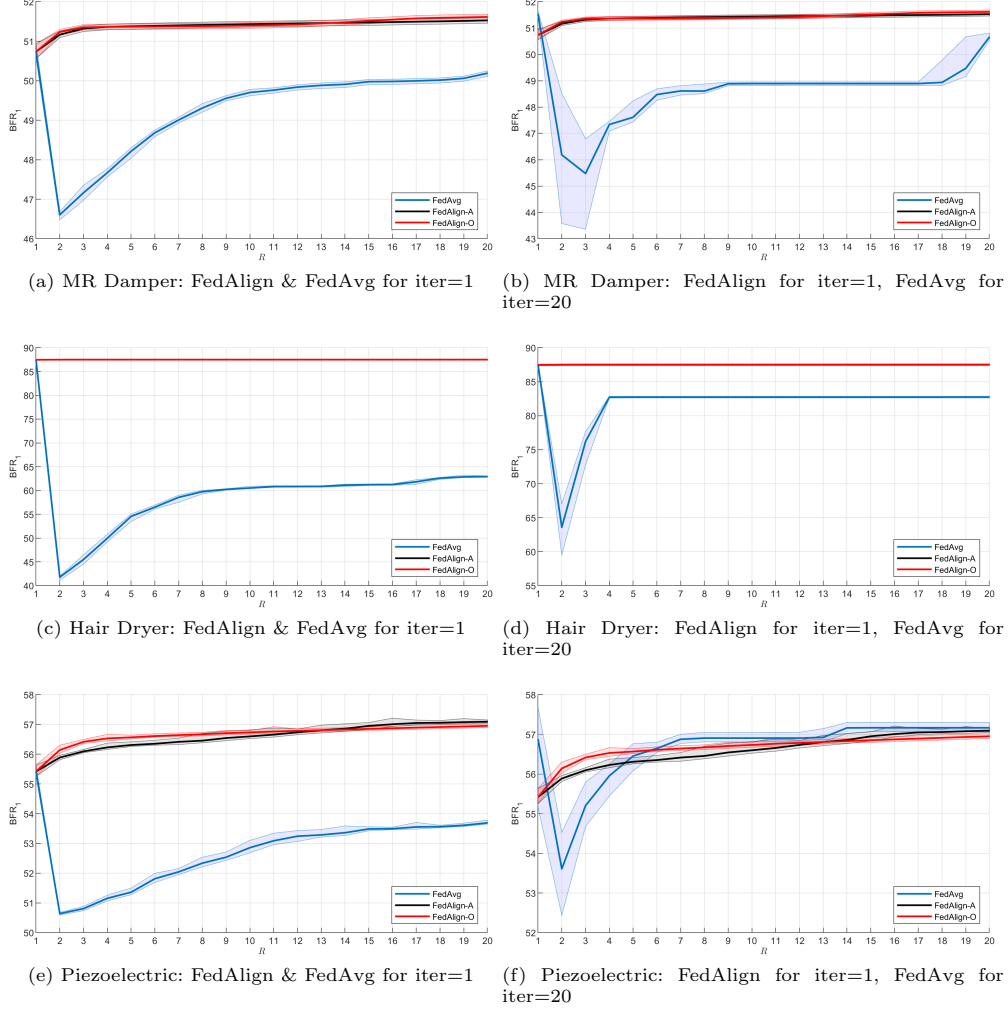
(a) MR Damper: FedAlign & FedAvg for iter=1

(b) MR Damper: FedAlign for iter=1, FedAvg for iter=20

(c) Hair Dryer: FedAlign & FedAvg for iter=1

(d) Hair Dryer: FedAlign for iter=1, FedAvg for iter=20

(e) Piezoelectric: FedAlign & FedAvg for iter=1

(f) Piezoelectric: FedAlign for iter=1, FedAvg for iter=20

Fig. 7 Comparison of FedAlign and FedAvg during training on real-world datasets: mean $\mathrm{BFR}^{(i)}$ across local workers with solid lines while minimum, and maximum $\mathrm{BFR}^{(i)}$ across local workers with shaded areas

5.4 Performance comparison study on real-world MIMO datasets

We conducted our performance evaluation on the following presplit datasets, each of which is already divided into training and test subsets, denoted by $D = \{D_{\mathrm{train}}, D_{\mathrm{test}}\}$.

- Steam Engine dataset [20] contains 451 samples with steam pressure and magnetization voltage as inputs ($nu = 2$) and generated voltage and rotational speed as the

outputs ($ny = 2$). D_{train} includes first 250 samples and D_{test} includes the remaining samples. To create diverse datasets $\forall W^i$, $\boldsymbol{v}_{1:K}^{(i)} \sim \mathcal{N}(0, 0.001^2 I_2)$ is sampled and added into D_{train}.

- The CD player data set [21] consists of 2,048 samples, with mechanical actuator forces ($nu = 2$) as input and arm tracking accuracy as output ($ny = 2$). D_{train} includes the first 1200 samples, and D_{test} consists of remaining samples. The dataset is normalized to achieve zero mean and unit variance. Noise $\boldsymbol{v}_{1:K}^{(i)} \sim \mathcal{N}(0, 0.05^2 I_2)$ is added to D_{train} for each W^i.

- The Evaporator dataset contains [22] 6305 samples with feed and vapor flows to the first evaporator stage and cooling water flow as inputs ($nu = 3$) and dry matter content, flow, and temperature of the outcoming product as outputs ($ny = 3$). The dataset is normalized to achieve zero mean and unit variance. D_{train} consists of the first 3000 samples, and D_{test} includes samples 3001-6000. Gaussian noise, $\boldsymbol{v}_{1:K}^{(i)} \sim \mathcal{N}(0, 0.1^2 I_3)$, is added to D_{train} for each W^i.

In this analysis, we set $iter = 1$ in FedAlign and $iter = \{1, 20\}$ in FedAvg as in real-world SISO datasets. We set $nx = 4$ for the Steam Engine and the Evaporator, and $nx = 2$ for the CD Player datasets. We utilized $\boldsymbol{u}_{1:K}^{(i)} \in D_{\text{test}}^i$ to generate $\tilde{\boldsymbol{x}}_{pseudo}^{(i)}$ in FedAlign-O. We set $\mu_1 = nx$ and constructed $M^{(i)} = P_1^{(i)}$ in FedAlign-A.

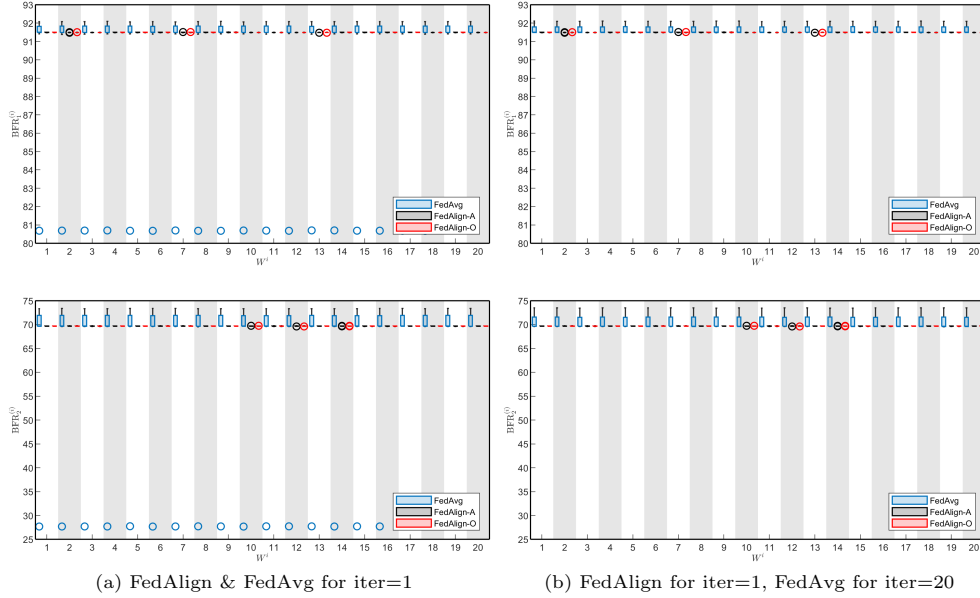(a) FedAlign & FedAvg for iter=1   (b) FedAlign for iter=1, FedAvg for iter=20

Fig. 8 Box plot comparison of FedAlign and FedAvg on the Steam Engine dataset for two outputs y_1 (top row) and y_2 (bottom row).

Table 5 reports the mean BFR values with standard errors, #UM and #F2L. Moreover, we evaluated the global SSM's SYSID performance against unseen data by
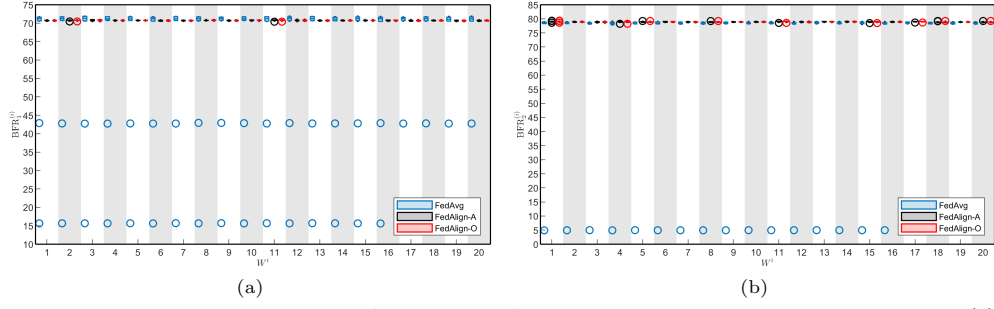
Fig. 9 Box plot comparison of FedAlign and FedAvg with iter = 1 on the CD Player dataset. (a) shows y_1, and (b) shows y_2.
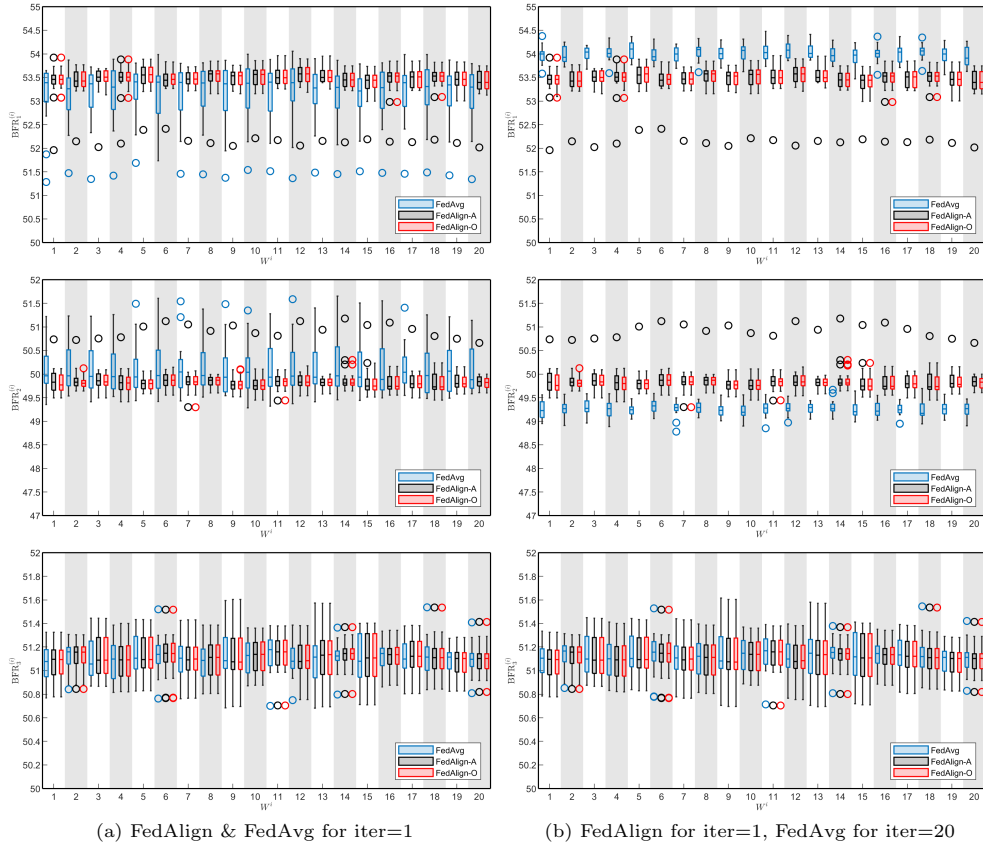

Fig. 10 Box plot comparison of FedAlign and FedAvg on the Evaporator dataset for three outputs y_1, y_2, and y_3. Each row shows a different output: y_1 (top row), y_2 (middle row), and y_3 (bottom row).

Table 5 Performance analysis over 20 experiments

			FedAvg		FedAlign-A	FedAlign-O
			iter=1	iter=20	iter=1	iter=1
Steam Engine	**BFR$_1$**	Train	91.09($\pm$2.46)	91.64($\pm$0.26)	91.48($\pm$0.002)	91.49($\pm$0.002)
		Test	89.31($\pm$1.20)	89.68($\pm$0.23)	89.81($\pm$0.001)	89.81($\pm$0.001)
	BFR$_2$	Train	68.53($\pm$9.74)	70.59($\pm$1.70)	69.68($\pm$0.008)	69.68($\pm$0.008)
		Test	46.25($\pm$6.78)	47.93($\pm$1.93)	49.13($\pm$0.005)	49.14($\pm$0.005)
	#UM		0	0	0	0
	#F2L		0	0	0	0
CD Player	**BFR$_1$**	Train	65.27($\pm$16.17)	-	70.71($\pm$0.04)	70.71($\pm$0.04)
		Test	62.43($\pm$15.73)	-	66.91($\pm$0.02)	66.91($\pm$0.02)
	BFR$_2$	Train	72.90($\pm$20.42)	-	78.90($\pm$0.03)	78.90($\pm$0.03)
		Test	73.20($\pm$19.48)	-	79.10($\pm$0.01)	79.10($\pm$0.01)
	#UM		6	20	0	0
	#F2L		1	0	0	0
Evaporator	**BFR$_1$**	Train	53.16($\pm$0.58)	54.01($\pm$0.05)	53.43($\pm$0.31)	53.49($\pm$0.07)
		Test	46.54($\pm$0.38)	46.96($\pm$0.05)	46.76($\pm$0.16)	46.79($\pm$0.06)
	BFR$_2$	Train	50.11($\pm$0.50)	49.26($\pm$0.04)	49.86($\pm$0.25)	49.81($\pm$0.06)
		Test	45.42($\pm$1.04)	43.80($\pm$0.05)	44.72($\pm$0.47)	44.63($\pm$0.08)
	BFR$_3$	Train	51.11($\pm$0.03)	51.13($\pm$0.03)	51.11($\pm$0.03)	51.12($\pm$0.03)
		Test	54.40($\pm$0.06)	54.49($\pm$0.02)	54.45($\pm$0.03)	54.45($\pm$0.03)
	#UM		1	0	0	0
	#F2L		0	0	0	0

evaluating BFR using D_{test}. We demonstrated box plots BFR$^{(i)}$ values of FedAvg and FedAlign in Fig. 8 - Fig. 10 while we presented the BFR$^{(i)}$ during the communication rounds in Fig. 11 - Fig. 13. We observed that:

- For $iter = 1$, FedAlign evaluates higher BFR values with smaller deviations than FedAvg on the Steam Engine and CD Player datasets. As seen in Fig. 8a and Fig. 9, the outliers reduce the performance of FedAvg while increasing its variability. On the other hand, FedAvg performs on par with FedAlign on the Evaporator dataset, although FedAlign-O achieves the lowest standard deviation as shown in Fig. 10a.
- FedAvg slightly surpasses the FedAlign's performance with $iter = 20$ in the Steam Engine dataset while showing only minor improvements in the Evaporator dataset as illustrated in Fig. 8b and Fig. 10b. Nevertheless, FedAvg generates unstable global SSMs across all experiments on the CD Player dataset for $iter = 20$.
- Figures 11 - 13 illustrates that FedAvg experiences performance decreases at the initial communication rounds on all real-world MIMO datasets whereas FedAlign consistently preserves its performance, therefore providing faster convergence.
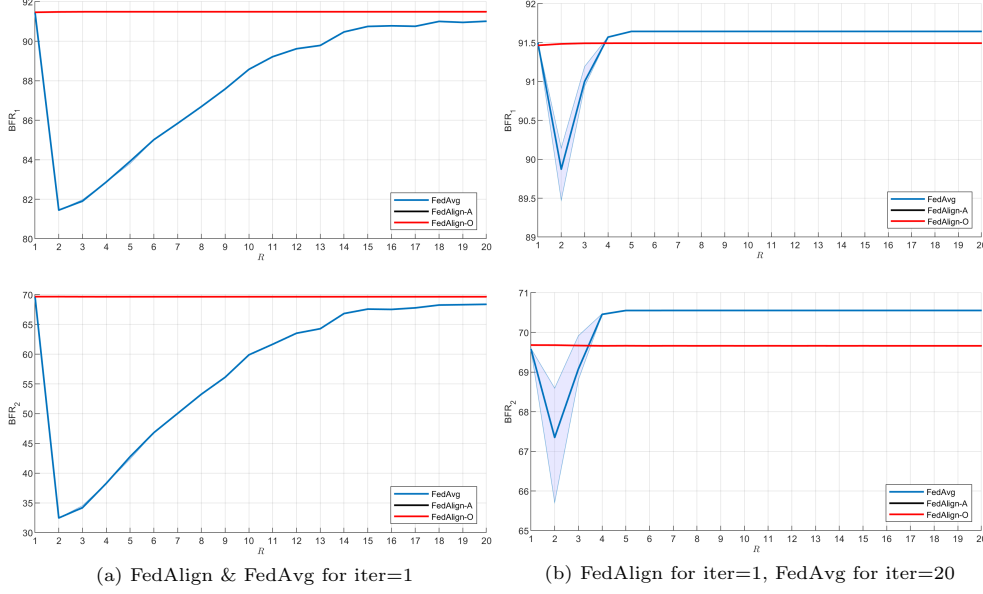
Fig. 11 Comparison of FedAlign and FedAvg training on Steam Engine dataset for two outputs y_1 (top row) and y_2 (bottom row): Mean $\text{BFR}^{(i)}$ across local workers (solid lines) and the minimum and maximum $\text{BFR}^{(i)}$ across local workers (shaded areas).
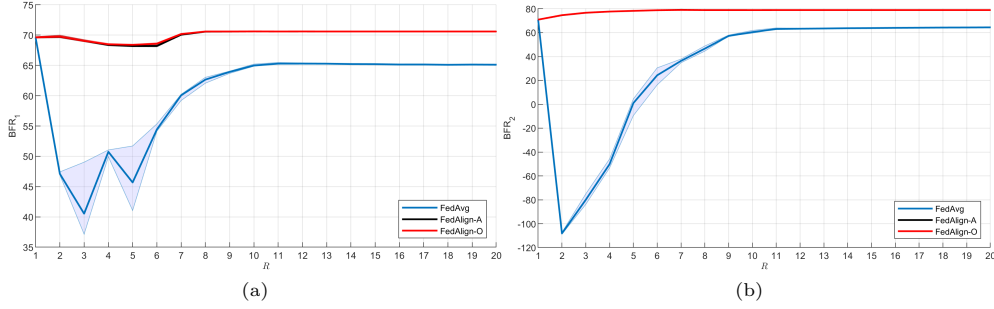

Fig. 12 Comparison of FedAlign and FedAvg with $iter = 1$ Training on CD Player dataset: Mean $\text{BFR}^{(i)}$ across local workers (solid lines) and the minimum and maximum $\text{BFR}^{(i)}$ across local workers (shaded areas). (a) shows y_1, and (b) shows y_2.

- FedAvg yields unstable global SSMs in the CD Player and Evaporator datasets. On the contrary, FedAlign enables enhanced stability of the global SSMs by aligning local parameter basins.
- Similar to the results on training data, FedAlign outperforms FedAvg against unseen data on all real-world MIMO datasets for $iter = 1$. FedAvg only evaluates higher test BFR on the Steam Engine dataset with the help of increased local iterations ($iter = 20$).
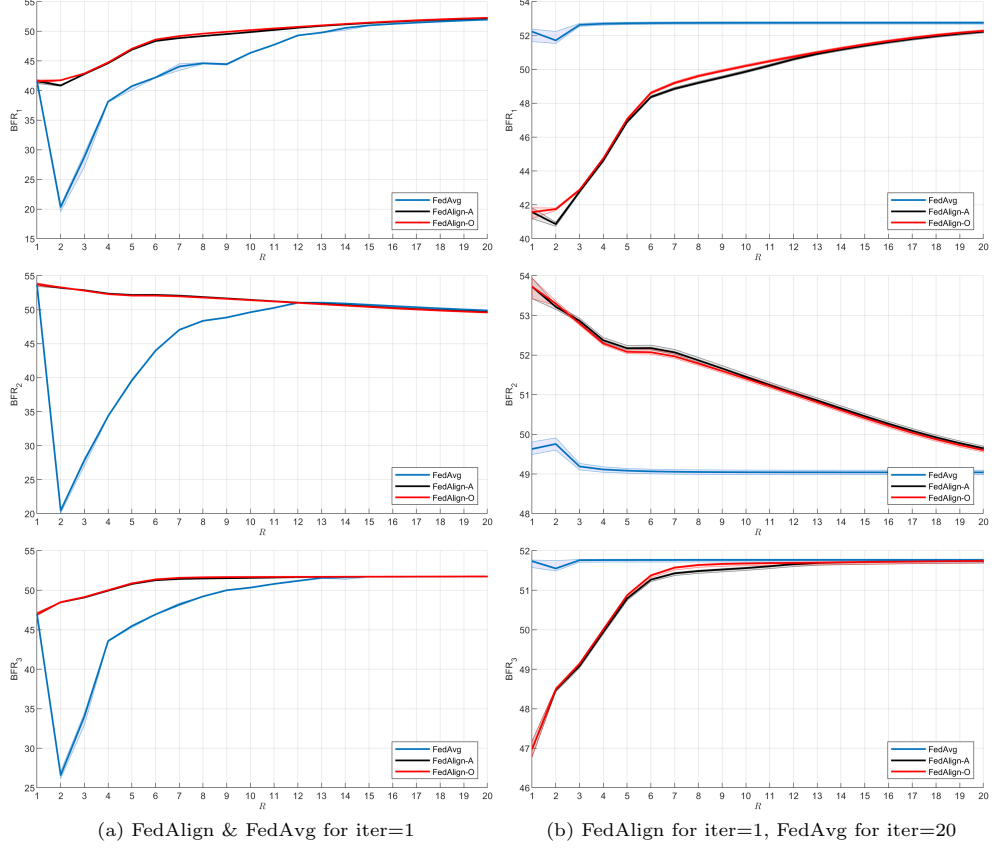
23

Fig. 13 Comparison of FedAlign and FedAvg during training on Evaporator dataset: mean BFR$^{(i)}$ across local workers with solid lines while minimum, and maximum BFR$^{(i)}$ across local workers with shaded areas. Each row shows a different output: y_1 (top row), y_2 (middle row), and y_3 (bottom row).

- FedAlign-A and FedAlign-O exhibit almost identical SYSID performance on all datasets indicating both methods successfully establish a common parameter basin in the center server.

To conclude, FedAlign efficiently aligns local parameter basins and provides high SYSID performance against both training and test data. Moreover, due to its local parameter basin alignment, FedAlign enhances the stability of global SSM and converges faster.

6 Conclusion and Future Work

In this paper, we propose FedAlign, an FL-SYSID framework designed to resolve alignment issues inherent in directly merging local SSMs via FedAvg. FedAlign overcomes these issues by aligning state representations of local SSMs through similarity transformation matrices. We developed two distinct methods in FedAlign to compute similarity

transformation matrices: FedAlign-A, where we exploit control theory to analytically derive similarity transformation matrices, and FedAlign-O, which formulates the alignment problem as an optimization task to estimate similarity transformation matrices. Experiments conducted on various real-world SISO and MIMO datasets demonstrate that FedAlign improves SYSID performance, convergence speed, and stability of the global SSM even with fewer local iterations or reduced order modeling, underlining the effectiveness of the proposed FL-SYSID framework.

The current FedAlign framework is limited to learning linear SSMs. Thus, in our future work, we aim to extend the FedAlign framework to handle nonlinear SSMs (based on neural networks), enabling it to address more complex SYSID tasks. We will also investigate incorporating uncertainty quantification into the alignment process to enhance the interpretability and reliability of the SYSID results.

Author contribution. All authors contributed to the study's conception and design. Material preparation, data collection, and analysis were performed by EK under the supervision of MG and TK. The manuscript was written by EK, MG, and TK. All authors read and approved the final manuscript.

Declarations

Conflict of interest. The authors declare that they have no conflict of interest to this work.

References

[1] Ljung, L.: Perspectives on system identification. Annual Reviews in Control **34**(1), 1–12 (2010)

[2] Keesman, K.J.: System Identification: an Introduction. Springer, ??? (2011)

[3] Chiuso, A., Pillonetto, G.: System identification: A machine learning perspective. Annual Review of Control, Robotics, and Autonomous Systems **2**(1), 281–304 (2019)

[4] Pillonetto, G., Aravkin, A., Gedon, D., Ljung, L., Ribeiro, A.H., Schön, T.B.: Deep networks for system identification: a survey. Automatica **171**, 111907 (2025)

[5] Dankers, A., Hof, P.M.J., Bombois, X., Heuberger, P.S.C.: Identification of dynamic models in complex networks with prediction error methods: Predictor input selection. IEEE Transactions on Automatic Control **61**(4), 937–952 (2016) https://doi.org/10.1109/TAC.2015.2450895

[6] Zhou, N., Pierre, J.W., Hauer, J.F.: Initial results in power system identification from injected probing signals using a subspace method. IEEE Transactions on

Power Systems **21**(3), 1296–1302 (2006) https://doi.org/10.1109/TPWRS.2006.879292

[7] Xin, L., Ye, L., Chiu, G., Sundaram, S.: Identifying the dynamics of a system by leveraging data from similar systems. In: American Control Conference, pp. 818–824 (2022)

[8] Zhang, T.T., Kang, K., Lee, B.D., Tomlin, C., Levine, S., Tu, S., Matni, N.: Multitask imitation learning for linear dynamical systems. In: Learning for Dynamics and Control Conference, pp. 586–599 (2023)

[9] Papusha, I., Lavretsky, E., Murray, R.M.: Collaborative system identification via parameter consensus. In: American Control Conference, pp. 13–19 (2014)

[10] Wang, H., Toso, L.F., Anderson, J.: Fedsysid: A federated approach to sample-efficient system identification. In: Learning for Dynamics and Control Conference, pp. 1308–1320 (2023)

[11] Toso, L.F., Wang, H., Anderson, J.: Learning personalized models with clustered system identification. In: IEEE Conference on Decision and Control, pp. 7162–7169 (2023). https://doi.org/10.1109/CDC49753.2023.10383950

[12] Keçeci, E., Güzelkaya, M., Kumbasar, T.: A novel federated learning framework for system identification. In: International Artificial Intelligence and Data Processing Symposium, pp. 1–6 (2024). https://doi.org/10.1109/IDAP64064.2024.10710886

[13] Ainsworth, S., Hayase, J., Srinivasa, S.: Git re-basin: Merging models modulo permutation symmetries. In: International Conference on Learning Representations (2023)

[14] McMahan, B., Moore, E., Ramage, D., Hampson, S., Arcas, B.A.: Communication-efficient learning of deep networks from decentralized data. In: Artificial Intelligence and Statistics, pp. 1273–1282 (2017)

[15] Wisassakwichai, C., Phaochoo, P.: Range space and similarity transformation using symbolic mathematics in python. IEEE Access **12**, 182788–182798 (2024) https://doi.org/10.1109/ACCESS.2024.3510632

[16] Bay, J.: Fundamentals of linear state space systems (1999)

[17] Wang, J., Sano, A., Chen, T., Huang, B.: Identification of hammerstein systems without explicit parameterisation of non-linearity. International Journal of Control **82**(5), 937–952 (2009)

[18] Aguilar, C.Z., Gómez-Aguilar, J., Alvarado-Martínez, V., Romero-Ugalde, H.: Fractional order neural networks for system identification. Chaos, Solitons &

Fractals **130**, 109444 (2020)

[19] The MathWorks Inc.: Piezoelectric Actuator Model Identification Using Machine Learning. The MathWorks Inc., Natick, Massachusetts, United States (2024). https://www.mathworks.com/help/ident/ug/machine-learning-based-identification-of-piezoelectric-actuator.html

[20] The MathWorks Inc.: Analyze Data in Multivariable Systems and Identify Models. The MathWorks Inc., Natick, Massachusetts, United States (2024). https://www.mathworks.com/help/ident/ug/dealing-with-multi-variable-systems-identification-and-analysis.html

[21] Van Den Hof, P.M., Schrama, R.J.: An indirect method for transfer function estimation from closed loop data. Automatica **29**(6), 1523–1527 (1993)

[22] Zhu, Y., Overschee, P., Moor, B., Ljung, L.: Comparison of three classes of identification methods. IFAC Proceedings Volumes **27**(8), 169–174 (1994)